Algorithm of Impact Point Prediction for Intercepting Reentry Vehicles

Cheng-Yu Liu

Lee-Ming Institute of Technology, Taipei, 243, Taiwan, People's Republic of China

and

Chiun-Chien Liu and Pan-Chio Tuan

Chung Cheng Institute of Technology, Tao Yuan, 335, Taiwan, People's Republic of China

ABSTRACT

Intercepting reentry vehicles is difficult because these move nearly at hypersonic speeds that traditional interceptors cannot match. Counterparallel guidance law was developed for defending a high speed target that guides the interceptor to intercept the target at a 180° aspect angle. When applying the counterparallel guidance law, it is best to predict the impact point before launch. Estimation and prediction of a reentry vehicle path are the first steps in establishing the impact point prediction algorithm. Model validation is a major challenge within the overall trajectory estimation problem. The adaptive Kalman filter, consising of an extended Kalman filter and a recursive input estimator, accurately estimates reentry vehicle trajectory by means of an input estimator which processes the model validation problem. This investigation presents an algorithm of impact point prediction for a reentry vehicle and an interceptor at an optimal intercept altitude based on the adaptive Kalman filter. Numerical simulation using a set of data, generated from a complicated model, verifies the accuracy of the proposed algorithm. The algorithm also performs exceptionally well using a set of flight test data. The presented algorithm is effective in solving the intercept problems.

Keywords: Reentry vehicle, trajectory estimation, input estimation, adaptive Kalman filter, impact point prediction, counterparallel guidance law

NOMENCLATURE

C_b	Ballistic coefficient
C_{D0}	Zero-lift drag coefficient
g	Gravity
G_i	6×6 Gain matrix
H, I	6×6 Identity matrix
k	Starting index of input
K_{n+1}	6×6 Kalman gain matrix
$P_{k+l/k+l-1}$	6×6 Covariance matrix of the predicted state
Q	6×6 Covariance matrix of process noise
R	6×6 Covariance matrix of measurement noise
r	Upper limit of the acceptance region
s	Stopping index of input

S	Reference area of the reentry vehicle
S_I	Flight range of the interceptor
t^*	Flight time
t_b	Time to terminate booster of the interceptor
t_l	Time to launch interceptor
t_p	Time to predict impact point
t_s	Time to head on the reentry vehicle
t_{st}	Upper limit of confidence interval
V_I	Velocity of the interceptor
V_i	6×6 Covariance matrix of the estimated input
V_{ii}	The ii^{th} element of V_i
W	Weight of the reentry vehicle
u_4, u_5, u_6	Unmodelled accelerations
v_0, v_b, v_s	Velocity constants
v_x, v_y, v_z	Velocity components
(v_x^*, v_y^*, v_z^*)	Impact point in velocity
x, y, z	Positions
(x^*, y^*, z^*)	Impact point in position
z^*	Optimal intercept altitude
Δt	Sampling period
ρ	Air density
ζ	6×1 Process noise vector
ε	6×1 Measurement noise vector
$v_i(j)$	Innovation of the ith state at $t = j\Delta t$

1. INTRODUCTION

The reentry vehicle (RV) flies at very high velocity, especially during the reentry phase, with speed reaching up to 10 Mach. The major difficulty in intercepting a reentry vehicle during the reentry phase, is that the velocity of a traditional interceptor, which is below 4.5 Mach, usually is significantly lower than that of a reentry vehicle. The conventional guidance laws such as pursuit, proportional navigation, etc thus become useless. Consequently, the counterparallel guidance law was developed for defending very high speed targets that navigate an interceptor along the trajectory of a target with

180° aspect angle[1]. Restated, the counterparallel guidance law guides an interceptor to collide head-on with the reentry vehicle. The impact point is thus defined as the intersection of the predicted trajectory of the reentry vehicle and counterparallel path of the interceptor. Accordingly, the impact point needs to be predicted to determine the launch time and the guidance parameters of the interceptor. An online, fast, and precision estimation and prediction method is required to accurately forecast the impact point.

The key issue in trajectory estimation problem is the model validation which focuses on the model error between the physical system and the mathematical model. Model error generally is induced by simplifying assumptions, manoeuvre, and unpredictable external forces in flight, parameter uncertainty, and by other sources. Measurable quantities in the mathematical model to be identified are also required and would make the problem worse if a precision radar is the only data source provider. The effects of the model error are considered extra input in the mathematical model for compensating and reducing estimation errors.

Chang[2], *et al.* designed an online filter for a manoeuvring reentry vehicle based on the augmented Kalman filter[2]. Position, velocity, drag force, and manoeuvre forces yield the augmented state vector and the estimation is performed using an extended Kalman filter(EKF). However, the proposed filter performance deteriorates for a non-manoeuvring vehicle. Manohar and Krishnan[3] reconstructed rocket trajectory using a differential corrections method whose measurements are beyond what a single radar can measure[3]. A simple model with the unmodelled acceleration input seems applicable for online trajectory estimation if a recursive determination of input is well-defined.

Least-squares methods have been successfully used to estimate the input for solving tracking problems[4-6], initial levelling problems in strapped-down inertial navigation[7,8], and inverse heat conduction problems[9,10]. Lee and Liu[11] proposed a method based on the EKF with a recursive input estimator, named the adaptive Kalman filter (AKF), for executing online

trajectory estimation for a reentry vehicle[11,12]. The robustness and accuracy of this method have been verified by simulation and flight tests. The method developed by Lee and Liu[11] is thus suitable for application to the impact point prediction problem. This investigation presents an algorithm to accurately predict the impact point for the interceptor and the reentry vehicle at an optimal altitude using the AKF. The trajectory of the reentry vehicle is predicted using the AKF. The flight path of the interceptor is approximated by the three straight lines based on the counterparallel guidance law. The impact point then can be determined using a constraint of optimal altitude that provides an excellent manoeuvrability. The increased accuracy is demonstrated by numerical simulation using data from a model with six degrees of freedom (6-DOFs) and flight test using data from an experiment.

This study formulates a model for a reentry vehicle and details an AKF that can quickly and accurately estimate trajectory in terms of the position, velocity, and flight time. An algorithm for predicting the impact point at an optimal intercept altitude is presented. Simulation and flight test results validate that the proposed algorithm provides accurate impact point prediction. The proposed algorithm is suitable for application to the reentry vehicle intercept problem.

2. DYNAMIC MODEL

Consider a vehicle in the reentry phase over a flat, nonrotating earth as illustrated in Fig. 1. Assume the reentry vehicle to be a point mass with constant weight following a ballistic trajectory in which two types of significant forces, drag and gravity, act on the reentry vehicle. Extra forces are induced by model error when assumptions are violated or the reentry vehicle undertakes a manoeuvre. The manoeuvring reentry vehicle model during reentry phase in radar coordinate (O_R, X_R, Y_R, Z_R) centred at the radar site can be expressed as

$$\&_x = -\frac{\rho v^2}{2C_b} g \cos\gamma_1 \sin\gamma_2 + u_4 \tag{1}$$

$$\&_y = -\frac{\rho v^2}{2C_b} g \cos\gamma_1 \cos\gamma_2 + u_5 \tag{2}$$

$$\&_z = \frac{\rho v^2}{2C_b} g \sin\gamma_1 - g + u_6 \tag{3}$$

where

$$C_b = \frac{W}{S C_{D0}}$$

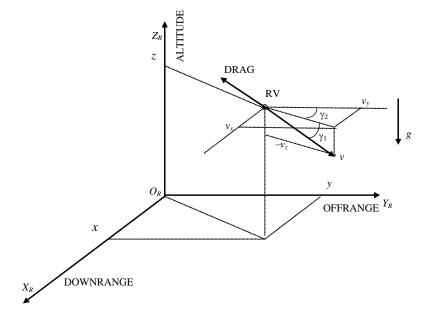**Figure 1. Reentry vehicle flight geometry**

$$\gamma_1 = \tan^{-1}(-\frac{v_z}{\sqrt{v_x^2 + v_y^2}})$$

$$\gamma_2 = \tan^{-1}(\frac{v_x}{v_y})$$

where ρ stands for air density and is a function of altitude[13]. The well-known normal gravity model is considered since the reentry vehicle generally flies over several hundred kilometers height[14].

Let the state vector be

$$X = [x_1\ x_2\ x_3\ x_4\ x_5\ x_6]^T = [x\ y\ z\ v_x\ v_y\ v_z]^T \quad (4)$$

The nonlinear state equation can be written as

$$\dot{X} = F(X) + \varphi u + I_{6\times6}\zeta \quad (5)$$

where

$$F(X) = \begin{bmatrix} x_4 \\ x_5 \\ x_6 \\ -\dfrac{\rho}{2C_b}(x_4^2 + x_5^2 + x_6^2)g\cos\gamma_1\sin\gamma_2 \\ -\dfrac{\rho}{2C_b}(x_4^2 + x_5^2 + x_6^2)g\cos\gamma_1\cos\gamma_2 \\ \dfrac{\rho}{2C_b}(x_4^2 + x_5^2 + x_6^2)g\sin\gamma_1 - g \end{bmatrix}$$

$$\varphi = \begin{bmatrix} 0_{3\times3} & 0_{3\times3} \\ 0_{3\times3} & I_{3\times3} \end{bmatrix}$$

$$u = \begin{bmatrix} 0 & 0 & 0 & u_4 & u_5 & u_6 \end{bmatrix}^T$$

An accurate phased array radar is taken for detecting the reentry vehicle. Position and velocity of the reentry vehicle are measured and filtered, respectively. The equation of measurement is:

$$Z = HX + \varepsilon \quad (6)$$

where ε is the measurement noise vector and is assumed to be normally distributed with mean zero and variance R. Equations (5) and (6) form the dynamic equations for the vehicle during reentry.

3. RECURSIVE INPUT ESTIMATION

The predicted and updated state vectors of the EKF from $t = n\Delta t$ to $t = (n+1)\Delta t$, $n = 0,1,2,...$, under a known input vector u_n at $t = n\Delta t$ are respectively given[15] as

$$\hat{X}_{n+1/n} = \varphi_n \hat{X}_{n/n} + \varphi u_n \quad (7)$$

$$\hat{X}_{n+1/n+1} = \hat{X}_{n+1/n} + K_{n+1}(Z_{n+1} - H\hat{X}_{n+1/n}) \quad (8)$$

where Z_{n+1} denotes radar measurements at $t = (n+1)\Delta t$, and the transition matrix.

$$\varphi_n = I_{6\times6} + \frac{\partial F(X)}{\partial X}\bigg|_{X=\hat{X}_{n/n}} \Delta t$$

K_{n+1}, $P_{n+1/n}$ and $P_{n+1/n+1}$ are the Kalman gain and covariance matrices. An input estimation algorithm of u_n is given as follows:

Let $\overline{X}_{n+1/n+1}$ be the updated state for the EKF with no input at $t = (n+1)\Delta t$. For simplicity, denote $\hat{X}_{n+1} = \hat{X}_{n+1/n+1}$, $\overline{X}_{n+1} = \overline{X}_{n+1/n+1}$, and define $M_{n+1} = (I - K_{n+1}H)\varphi_n$, $N_{n+1} = (I - K_{n+1}H)\varphi$. Assume that the abrupt deterministic input are applied during $k\Delta t \le t \le (k+s)\Delta t$, then one gets:

$$u = \begin{cases} 0 & t < k\Delta t, t > (k+s)\Delta t \quad k,s > 0 \\ u_{k+l} & k\Delta t \le t \le (k+s)\Delta t \quad l = 0,1,2,...,s \end{cases} \quad (9)$$

where u_{k+l} is a constant vector over the sampling interval. Then $\hat{X}_k = \overline{X}_k$ during $t \le k\Delta t$. Define the measurement residual for the EKF with no input to be $\overline{Z}_{k+l} = Z_{k+l} - H\overline{X}_{k+l}$.

The recursive least-squares input estimator can be derived as[11,12]

$$\hat{u}_{k+l-1} = \hat{u}_{k+l-2} + G_{k+l}\left(\hat{Y}_{k+l} - \Phi_{k+l}\hat{u}_{k+l-2}\right)$$

$$l = 0,1,2,...,s \quad (10)$$

where

$$\hat{Y}_{k+l} = \overline{Z}_{k+l} - HM_{k+l}\Delta\hat{X}_{k+l-1}$$

$$\Phi_{k+l} = HN_{k+l}$$

$$\Delta\hat{X}_{k+l-1} = M_{k+l}\Delta\hat{X}_{k+l-2} + N_{k+l}\hat{u}_{k+l-2}$$

and the gain G_i and variance of $\hat{u}_i$, V_i, are:

$$G_{k+l} = V_{k+l-1}\Phi_{k+l}\xi^{-1}$$

$$V_{k+l-1} = V_{k+l-2} - V_{k+l-2}\Phi_{k+l}^T[\Phi_{k+l}V_{k+l-2}\Phi_{k+l}^T + \xi]^{-1}\Phi_{k+l}V_{k+l-2}$$

$$\xi = R + HP_{k+l/k+l-1}H^T$$

In Eqn (10), k and s represent the starting and stopping indices of the system input, respectively, can be determined by testing. The test for detection of input is expressed[11,12] as

$$\left|\frac{\hat{u}_i}{\sqrt{V_{ii}}}\right| > t_{st} \quad \text{existence of } u_i \text{ for } i = 4,5,6 \quad (11)$$

otherwise u_i is absent. The value of t_{st} can be determined by inspecting the cumulative normal distribution table for a preset confidence coefficient, $1-\alpha$.

4. ADAPTIVE KALMAN FILTER

By incorporating the estimated input into the EKF, the predicted and the updated states at time interval $k\Delta t \leq t \leq (k+s)\Delta t$ are:

$$\hat{X}_{k+l/k+l-1}^v = \varphi_{k+l-1}\hat{X}_{k+l-1/k+l-1}^v + \varphi\hat{u}_{k+l-1} \quad (12)$$

$$\hat{X}_{k+l/k+l}^v = \hat{X}_{k+l/k+l-1}^v + K_{k+l}^v(Z_{k+l} - H\hat{X}_{k+l/k+l-1}^v) \quad (13)$$

The Kalman gain becomes:

$$K_{k+l}^v = P_{k+l/k+l-1}^v H^T (HP_{k+l/k+l-1}^v H^T + R)^{-1} \quad (14)$$

with the covariance matrices of $\hat{X}_{k+l/k+l-1}^v$ and

$\hat{X}_{k+l/k+l}^v$ at $k\Delta t \leq t \leq (k+s)\Delta t$ being

$$P_{k+l/k+l-1}^v = P_{k+l/k+l-1} + \varphi_{k+l-1}L_{k+l}\varphi_{k+l-1}^T + \varphi V_{k+l-1}\varphi^T \quad (15)$$

$$P_{k+l/k+l}^v = (I - K_{k+l}^v H)P_{k+l/k+l-1}^v \quad (16)$$

where

$$L_{k+1} = 0 \quad L_{k+2} = N_{k+2}V_k N_{k+2}^T$$

$$L_{k+l} = \sum_{j=1}^{l-1}(\prod_{i=1+j}^{l}M_{k+i-1})N_{k+j}V_{k+j-1}N_{k+j}^T(\prod_{i=1+j}^{l}M_{k+i-1}^T)$$

$$= M_{k+l-1}L_{k+l-1}M_{k+l-1}^T$$

For time beyond the interval $t < k\Delta t$ and $t > (k+s)\Delta t$, state estimation can also be based upon the original EKF. Note that the initial states and covariance matrices at $t > (k+s)\Delta t$ are reinitiated by $\hat{X}_{k+s/k+s}^v$ and $P_{k+s/k+s}^v$. Equations (10) to (16) form the adaptive Kalman filter (AKF) and Fig. 2 schematically depicts the proposed filter.

5. PREDICTION OF IMPACT POINT

The impact point is geometrically defined as the intersection between the predicted reentry vehicle trajectory and the interceptor flight path. At the time to predict impact point, t_p, the reentry vehicle trajectory at $t \geq t_p$ can be predicted from Eqns (1) to (3) with $u_4 = u_5 = u_6 = 0$ and initial state $\hat{X}_{n/n}^v$ where $n = t_p/\Delta t$.

The interceptor flight path depends on the interception strategy. The major problem for intercepting the reentry vehicle during the reentry phase is that the velocity of the reentry vehicle can reach 10 Mach, significantly exceeding the most conventional interceptors whose maximum speed is below 4.5 Mach. Most traditional pursuit and proportional navigation guidance laws thus are unsuitable for such interceptions. The counterparallel guidance law was designed to keep a head-on correlation between the reentry
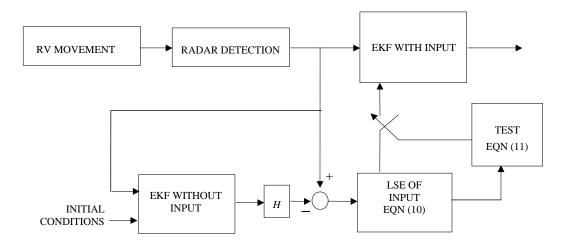
Figure 2. Mechanism of the adaptive Kalman filter scheme

vehicle and the interceptor. This law directs the interceptor along the path with a 180° aspect angle to the predicted trajectory of the reentry vehicle in the shortest time without excessive velocity loss. The flight path of the interceptor can then be roughly divided into three segments, from launch point O to P_1, from P_1 to P_2, and from P_2 to P^*, as illustrated in Fig. 3. In the first segment, process control phase, required velocity and attitude should be achieved. The interceptor then is refracted to point P_2, entering the path parallel with but facing the approaching reentry vehicle and is guided to the impact point using midcourse and terminal guidances. The velocities at each time intervals are approximated empirically as

$$V_I(t) = v_0 \times \left(\frac{t}{t_b}\right) \qquad 0 \le t \le t_b \qquad (17)$$

$$V_I(t) = v_0 + v_b \times \left(\frac{t - t_b}{t_s - t_b}\right) \qquad t_b \le t \le t_s \qquad (18)$$

$$V_I(t) = v_b - v_s \times \left(\frac{t - t_s}{t_0}\right) \qquad t_s < t \qquad (19)$$

where $t_0 = 3$s. The related flight ranges are then obtained as

$$S_I(t) = 0.5 \times V_I(t) \times t \qquad 0 \le t \le t_b \qquad (20)$$

$$S_I(t) = 0.5 \times V_I(t_b) \times t_b + 0.5 \times [V_1 + V_I(t)] \times (t - t_b)$$
$$0 \le t \le t_b \qquad (21)$$

$$S_I(t) = V_0 \times t_b + 0.5 \times [V_1 + V_I(t_s)] \times (t_s - t_b)$$
$$+ 0.5 \times [V_I(t_s) + V_I(t)] \times (t - t_s) \qquad t_s < t$$
$$(22)$$

where $V_0 = 0.5$ m/s and $V_1 = 1$ m/s. The values of v_0, v_b, v_s, t_b, and t_s greatly rely on the interceptor properties and are determined by simulation in adavance. The impact point, P^*, is the intersection of the estimated reentry vehicle trajectory and the simplified interceptor flight path given in Eqns (17) to (22) at a certain flight time t^*.

The criterion of the impact point prediction algorithm is that the flight time t^* from O to P^* should equal to the time spent by the reentry vehicle from its position at t_p to P^*. Since the manoeuvrability of the interceptor decreases at altitude, the maximum interceptable altitude is limited to a certain range, for example, 5 km to 20 km. Consequently, the impact point is restricted to an optimal intercept altitude z^* to ensure excellent manoeuverability of the interceptor. The steps of the algorithm associated with the AKF for predicting impact point at z^* are as follows:
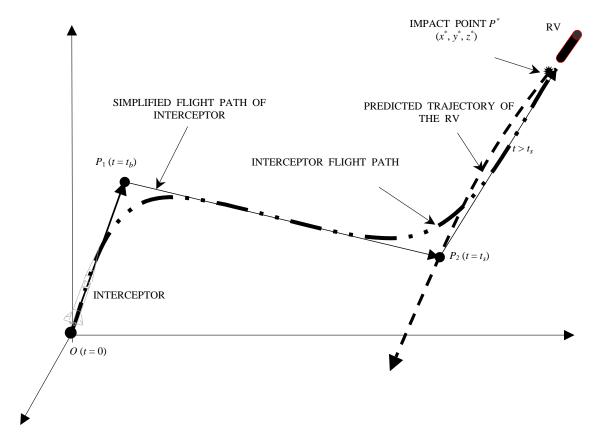
Figure 3. Interception strategy against the reentry vehicle

Step 1. Estimating the trajectory of the reentry vehicle using the AKF.

Step 2. Predicting the reentry vehicle position (x^*, y^*), velocity (v_x^*, v_y^*, v_z^*), and flight time t^* from its position at t_s to a given z^* based on the AKF.

Step 3. Calculating the flight time t_f of the interceptor from O to the point (x^*, y^*, z^*) from the simplified trajectory.

Step 4. If $t^* \leq t_f \leq t^* + \Delta t$ indicating that the interceptor and the reentry vehicle require the same flight time to reach the impact point (x^*, y^*, z^*), then the interceptor is launched at launch time, $t_l = t_p$. If $t_f > t^* + \Delta t$, return to *Step* 1. Otherwise, the interception fails.

The impact point prediction algorithm may be associated with other trajectory estimation methods.

6. SIMULATION & FLIGHT TEST

This section evaluates the algorithm associated with the AKF using simulation data and real flight data by comparing the prediction errors with two algorithms using the EKF and $\alpha-\beta$ filter[16] with position and velocity gains 0.488 and 0.108, respectively.

Case 1. *Simulation*

A 6-DOFs model of a flying vehicle is a set of equations of motion, including both translational and rotational motion. This model is more complicated than the 3-D model indicated in Eqns (1) to (3). In this case, a simulation analysis based on a set of data generated from a 6-DOFs model is utilised to compare prediction errors among these three algorithms. It is the mismatched case and would lead the mismatched filters. The simulated trajectory for a specific reentry vehicle is with the measurement noise which is generated from a verified radar

model. The whiteness test for trajectory estimation using the AKF and EKF is given first to show the consistency under this mismatched case. Let the time-average autocorrelation of the ith state up to $t = k\Delta t$ be[17]

$$\overline{\rho}_i = \sum_{j=1}^{k} v_i(j)v_i(j+1)[\sum_{j=1}^{k} v_i^2(j)\sum_{j=1}^{k} v_i^2(j+1)]^{-\frac{1}{2}} \quad (23)$$

For large enough k, $\overline{\rho}_i$ is, in view of the central limit theorem, normally distributed. The hypothesis that the correlation of the innovation sequence is zero, is accepted if the time-average autocorrelation is falling in the acceptance region, that is, $\overline{\rho}_i \in [-r, r]$ where $r = t_{st}/\sqrt{k}$. However, the mismatch would cause an unacceptable situation[17]. The distance between the time-average autocorrelation induced by the AKF or EKF and acceptable region becomes the key issue.

Figures 4 and 5 depict the time-average autocorrelation using the AKF and EKF under the

acceptance region with 95 per cent probability that is $t_{st} = 1.96$. Although the time-average autocorrelation induced by the AKF is outside the 95 per cent probability region, it approaches the region well and is much better than that by the EKF. The mismatch situation is improved by the input estimation definitely. The impact point prediction begins to predict after 10 s and the reentry vehicle reaches z^* at $t = 48$ s. Notably, the time t_p relates to the prediction accuracy and interceptor launch time. Accuracy increases with increasing t_p, providing an accurate impact point, but launch time, t_l, is delayed, curtailing the intercept range. Therefore, t_p is an independent variable.

The ballistic coefficient, C_b, is set at 9646.5 kg/m² in the simulation. Figures 6 to 11 display the flight time, position, and velocity prediction errors generated by the three algorithms using AKF, EKF, and $\alpha-\beta$ filter under 0.95 confidence coefficient, that is $\alpha = 0.05$.

For flight time prediction, the errors induced by the algorithm associated with the AKF keep in
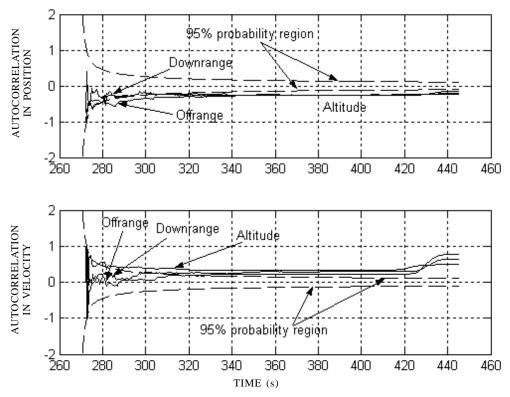

Figure 4. Time-average autocorrelation using the adaptive Kalman filter
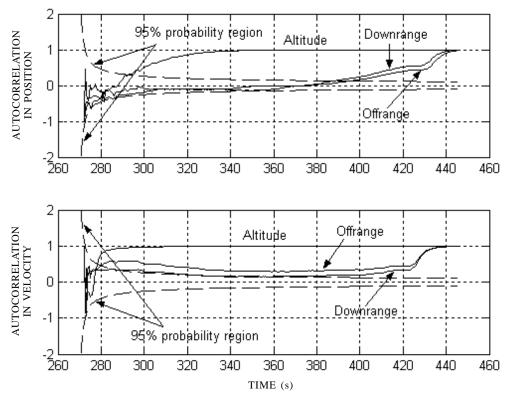
Figure 5. Time-average autocorrelation using the extended Kalman filter

±1s and approach zero as t_p grows. Moreover, the prediction errors generated by the algorithm using α−β filter are within ±8 s, and approach zero as t_p increases with large amplitudes. The EKF has the largest error among three approaches, of up to 23 s, but tends to converge over a longer period of time. For position prediction in X_R and Y_R, the AKF yields the smallest errors among the three methods, with a maximum of 2 km at t_p =18 s. The α−β filter offers an oscillated error curve with a maximum amplitude of 25 km in X_R and 15 km in Y_R, which is much larger than that of the AKF. Finally, the EKF has prediction errors within 15 km to 27 km in X_R and 10 km to 18 km in Y_R, but also tends to converge. The small errors of the AKF are easily corrected if the terminal guidance is used. The fluctuation of the prediction errors induced by the algorithm using α−β filter would result in unstable interception. Obviously, the prediction results of the algorithms using α−β filter and EKF are inadequate for interception.

Velocity prediction errors for the AKF are always bounded 0 m/s to 200 m/s. Meanwhile, for the α−β filter, the velocity prediction error curve also oscillates with a maximum amplitude of 280 m/s, 290 m/s, and 420 m/s in X_R, Y_R, and Z_R, respectively. The algorithm associated with EKF gives accurate predictions in X_R, Y_R, and Z_R. Table 1 lists the prediction errors of these three algorithms associated with the AKF, EKF, and α−β filter, without terminal guidance at launch time t_l = 29.0 s, t_l = 26.5 s, and

Table 1. Prediction error of impact point

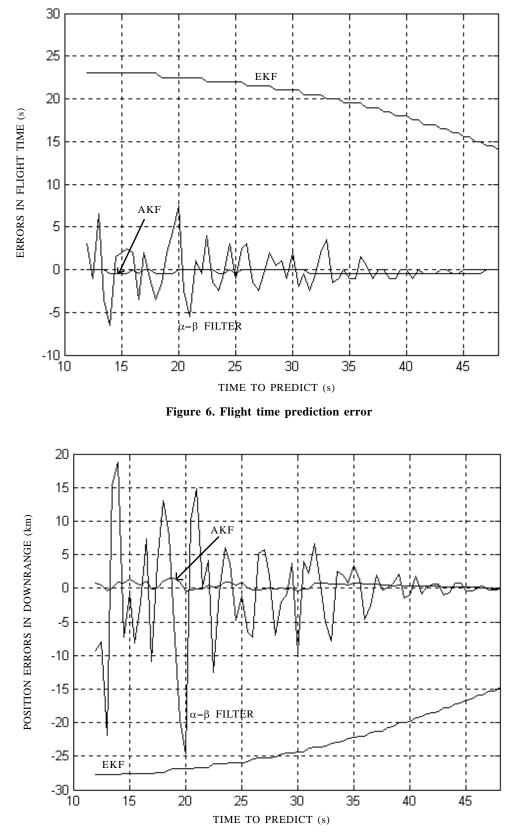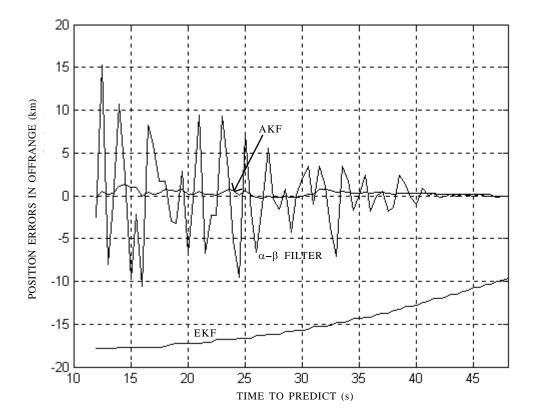| Type	Flight time (s)	Position X_R (km)	Position Y_R (km)	Velocity X_R (m/s)	Velocity Y_R (m/s)	Velocity Z_R (m/s)
AKF	0	0.28	0.40	85.70	62.30	106.50
α-β filter	3.50	15.42	0.92	200.30	151.80	256.50
EKF	21.50	25.55	16.44	27.60	13.70	229.10

Figure 6. Flight time prediction error

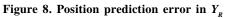**Figure 7. Position prediction error in X_R**

Figure 8. Position prediction error in Y_R

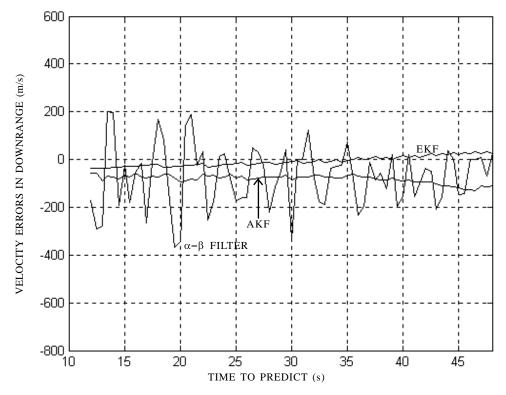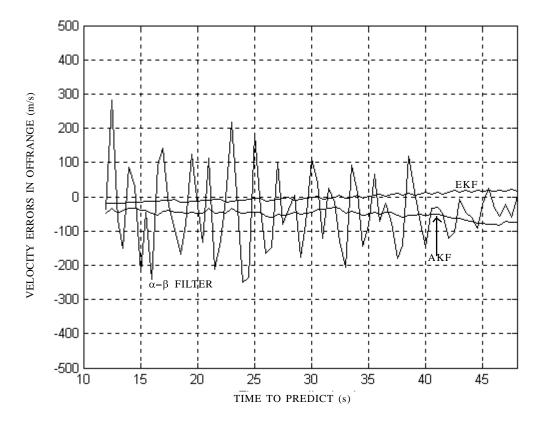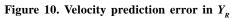**Figure 9. Velocity prediction error in X_R**

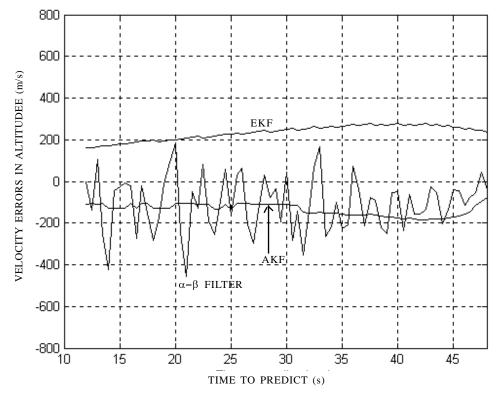**Figure 10. Velocity prediction error in Y_R**

Figure 11. Velocity prediction error in Z_R

t_l = 13.5 s, respectively. The position errors of 278.5 m in X_R, 396.5 m in Y_R and zero flight time error for the proposed algorithm are easily corrected by terminal guidance. The errors generated by the algorithm using EKF may be corrected if an excellent terminal guidance is included. The interceptor launched at t_l = 13.5 s provided by the α−β filter is too early that it causes a failed interception since the intercept range exceeds the designed range. This result is unacceptable unless the oscillated prediction error is improved. Therefore, the proposed algorithm associated with the AKF for impact point prediction provides accurate prediction and satisfies the requirements of midcourse guidance.

Case 2. Real Flight Test

Two sets of data were gathered in a flight test. The first data set, called the measured trajectory, was detected by a precision radar with sampling time 0.5 s. Meanwhile, the other, named the INS trajectory which was the closest to real trajectory, was measured and transmitted by onboard inertial

sensors and transmitters. The INS trajectory is considered the true trajectory of the reentry vehicle. The prediction error is then defined as the difference between the predicted impact point and the INS trajectory at an optimal altitude z*.

Let C_b = 9646.5 kg/m², and α = 0.05. The measured trajectory from t = 55.0 s to 126.7 s was adopted and the reentry vehicle reached an altitude of z^* at t = 103.5 s. Figures 12 to 17 display the flight time, position and velocity prediction errors induced by the algorithms associated with the AKF, EKF, and α−β filter. The prediction errors induced by the proposed algorithm associated with the AKF converges with t_p increasing and performs well in predicting impact point. Moreover, the algorithm using EKF induces large prediction error, which is also illustrated by the simulation results. The algorithm using α−β filter provides oscillated prediction error curves with very large amplitudes. Similarly, the fluctuation of prediction error causes unstable predictions and creates difficulty in achieving interception. Obviously, the algorithms using EKF and α−β filter
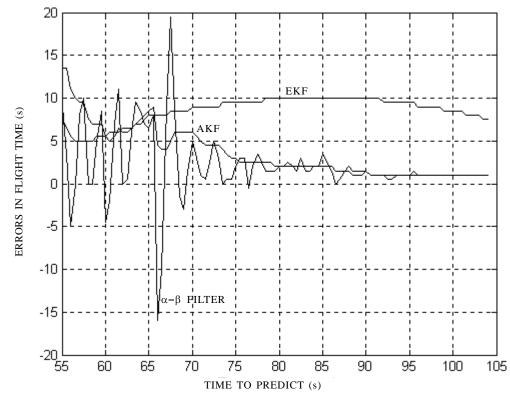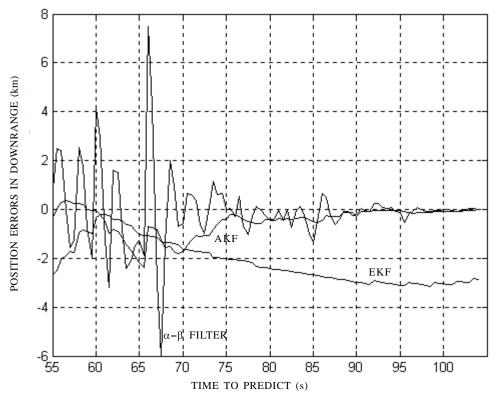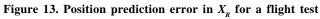

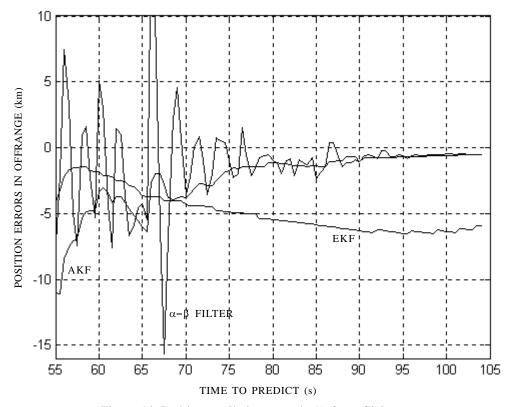**Figure 12. Flight time prediction error for a flight test**

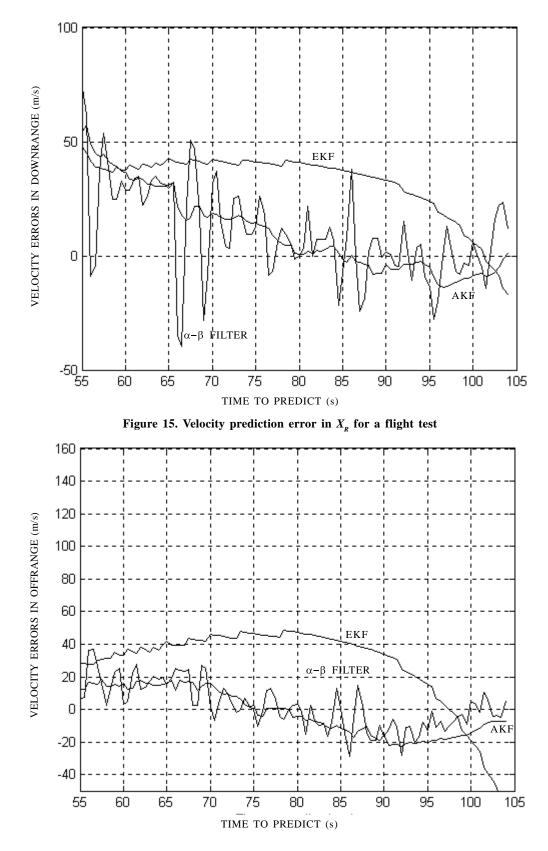**Figure 13. Position prediction error in X_R for a flight test**

Figure 14. Position prediction error in Y_R for a flight test

Figure 15. Velocity prediction error in X_R for a flight test

Figure 16. Velocity prediction error in Y_R for a flight test
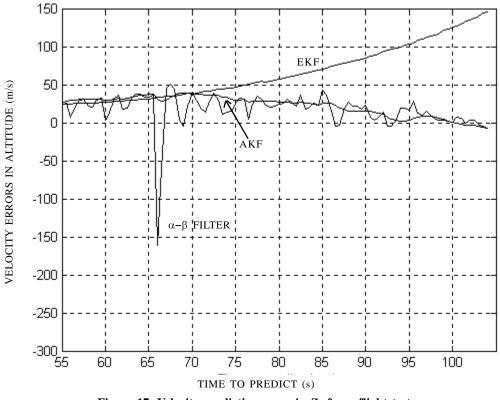
143

Figure 17. Velocity prediction error in Z_R for a flight test

Table 2. Prediction error of impact point for a flight test

	Flight time (s)	Position X_R (km)	Position Y_R (km)	Velocity X_R (m/s)	Velocity Y_R (m/s)	Velocity Z_R (m/s)
AKF	2.50	0.72	1.85	1.90	14.06	36.95

are unaccptable. Table 2 lists the prediction errors induced by the proposed algorithm with launch time $t_l = 85.5$ s. The small position prediction errors are easily corrected by terminal guidance. The proposed algorithm satisfies midcourse guidance requirements that leads the interceptor to fly in the tolerated basket to enter the terminal guidance phase.

7. CONCLUSIONS

This study presents an accurate algorithm of the impact point prediction for the interceptor and reentry vehicle at an optimal intercept altitude based on the AKF with a recursive input estimator. The proposed algorithm attempts to identify the intersection of the predicted trajectory of the reentry vehicle and the flight path of the interceptor. The predicted trajectory is obtained using the AKF which comprises an EKF and an input estimator with a detection

criterion. The flight path of the interceptor can be approximated by three straight lines from the launch point to the impact point, based on the counterparallel guidance law. The accuracy of the proposed algorithm is validated using simulation data generated from a model with 6-DOFs and flight data collected in the test. Small prediction errors induced by the proposed algorithm are easily corrected by terminal guidance. This investigation thus concludes that the proposed algorithm is worthy of further applications.

REFERENCES

1. Imado, F. & Kurodo, T. Optimal missile guidance system against a hypersonic target. AIAA-92-4531, 1992.

2. Chang, C.B.; Whiting, R.H. & Athans, M. On the state and parameter estimation for manoeuvring

reentry vehicles. *IEEE Trans. Automatic Cont.*, 1977, **AC-22**(1), 99-105.

3. Manohar, D.R. & Krishnan, S. Trajectory reconstruction during thrusting phase of rockets using differential corrections. *J. Guid. Cont. Dyn.*, 1985, **8**(3), 406-08.

4. Chan, Y.T. & Hu, A.G.C. A Kalman filter-based tracking scheme with input estimation. *IEEE Trans. Aerospace Elect. Syst.*, 1979, **AES-15**(2), 237-44.

5. Chan, Y.T.; Plant, J.B. & Bottomley, J. A Kalman tracker with a simple input estimator. *IEEE Trans. Aerospace Elect. Syst.*, 1982, **AES-18**(2), 235-41.

6. Bogler, P.L. Tracking a manoeuvring target using input estimation. *IEEE Trans. Aerospace Elect. Syst.*, 1987, **AES-23**(3), 298-10.

7. Liu, C.Y.; Lee, S.C. & Hou, W.T. Initial leveling using an adaptive Kalman filter. *J. Chung Cheng Inst. Technol.*, 1997, **25**(2), 147-62.

8. Lee, S.C. & Liu, C.Y. Fast automatic leveling subject to abrupt input. *IEEE Trans. Aerospace Elect. Syst.*, 1999, **AES-35**(3), 989-16.

9. Tuan, P.C.; Ji, C.C.; Fong, L.W. & Huang, W.T. An input estimation approach to online two-dimensional inverse heat conduction problem. *Num. Heat. Trans.*, (Part B) 1996, **29**, 345-63.

10. Tuan, P.C. & Fong, L.W. An IMM tracking algorithm with input estimation. *Int J. Syst. Sci.*, 1996, **27**(7), 629-39.

11. Lee, S.C. & Liu, C.Y. Trajectory estimation of reentry vehicles by use of online input estimation. *J. Guid. Cont. Dyn.*, 1999, **22**, 808-15.

12. Liu, C.Y.; Wang, H.M. & Tuan, P.C. Input estimation algorithms for reentry vehicle trajectory estimation. *Def. Sci. J.* 2005, **55**(4), 361-75.

13. Zarchan, P. Tactical and strategic missile guidance. American Institute of Aeronautics and Astronautics Inc, 1994, 363 p.

14. Siouris, G.M. Aerospace avionics system: A modern synthesis. Academic Press Inc, 1993. 460 p.

15. Gelb, A. Applied optimal estimation. *In* The M.I.T. Press, MA, 1974. pp. 107-12.

16. Kalata, P.R. The tracking index: A generalised parameter for $\alpha-\beta$ and $\alpha-\beta-\gamma$ target trackers. *IEEE trans. Aerospace Elect. Syst.*, 1984, **AES-20**(2), 174-81.

17. Bar-Shalom, Y.; Li, X.R. & Kirubarajan, T. Estimation with applications to tracking and navigation. John Wiley & Sons Inc, 2001.

Contributors

Dr Cheng-Yu Liu received his MS and PhD, both from the Chung Cheng Institute of Technology, Taiwan, in 1983 and 1998. He had worked at the Chung Shan Institute of Science and Technology from 1985 to 2002. Presently, he is Assist Professor in the Department of Electronic Engineering of the Lee-Ming Institute of Technology. His research areas include: System identification, control theory, tracking system, etc.

Mr Chiun-Chien Liu received his MS (Syst Engg) from the Chung Cheng Institute of Technology, Taiwan, in 2001. His major research interests include: Estimation theory, control theory applications, tracking system, etc.

Prof Pan-Chio Tuan received his BS(Syst Engg) in 1977 from the Chung Cheng Institute of Technology, Taiwan, MS(Mechanics and Dynamics) from the Ching Hwa University in 1981, and PhD in Mechanics from the North Carolina State University, USA, in 1991. He had served in Department of System Engineering at the Chung Cheng Institute of Technology, Taiwan, from 1981 to 2005. Presently, he is Professor in the Department of Computer Science and Information Engineering at the Nan Kai Institute of Technology, Taiwan. His areas of interest include: Estimation theory, tracking system, signal processing, etc.